

Geo-Congress 2026

GSP 377

Foundations, Retaining Structures, and Underground Engineering

Selected Papers from Geo-Congress 2026
Salt Lake City, Utah | March 9–12, 2026

Edited by

Jack Montgomery, Ph.D., P.E.
Brady R. Cox, Ph.D., P.E.

ASCE

G-I GEO-INSTITUTE

GEOTECHNICAL SPECIAL PUBLICATION NO. 377

GEO-CONGRESS 2026

FOUNDATIONS, RETAINING STRUCTURES, AND UNDERGROUND ENGINEERING

SELECTED PAPERS FROM SESSIONS OF GEO-CONGRESS 2026

March 9–12, 2026
Salt Lake City, Utah

SPONSORED BY

The Geo-Institute
of the American Society of Civil Engineers

EDITED BY
Jack Montgomery, Ph.D., P.E.
Brady R. Cox, Ph.D., P.E.

Published by the American Society of Civil Engineers

Published by American Society of Civil Engineers
1801 Alexander Bell Drive
Reston, Virginia, 20191-4382
www.asce.org/publications | ascelibrary.org

Any statements expressed in these materials are those of the individual authors and do not necessarily represent the views of ASCE, which takes no responsibility for any statement made herein. No reference made in this publication to any specific method, product, process, or service constitutes or implies an endorsement, recommendation, or warranty thereof by ASCE. The materials are for general information only and do not represent a standard of ASCE, nor are they intended as a reference in purchase specifications, contracts, regulations, statutes, or any other legal document. ASCE makes no representation or warranty of any kind, whether express or implied, concerning the accuracy, completeness, suitability, or utility of any information, apparatus, product, or process discussed in this publication, and assumes no liability therefor. The information contained in these materials should not be used without first securing competent advice with respect to its suitability for any general or specific application. Anyone utilizing such information assumes all liability arising from such use, including but not limited to infringement of any patent or patents.

ASCE and American Society of Civil Engineers—Registered in U.S. Patent and Trademark Office.

Photocopies and permissions. Permission to photocopy or reproduce material from ASCE publications can be requested by sending an e-mail to permissions@asce.org or by locating a title in ASCE's Civil Engineering Database (http://cedb.asce.org) or ASCE Library (http://ascelibrary.org) and using the "Permissions" link.

Errata: **Errata, if any, can be found at https://doi.org/10.1061/9780784486726**

Copyright © 2026 by the American Society of Civil Engineers.
All Rights Reserved.
ISBN 978-0-7844-8672-6 (PDF)
Manufactured in the United States of America.

Preface

This is the third volume of seven Geotechnical Special Publications (GSPs) containing papers from Geo-Congress 2026: Geo Tools, Technologies, and Techniques in an Environment of Change, held in Salt Lake City, Utah, on March 9-12, 2026. Notably, this conference marks the 30th anniversary of the Geo-Institute. The conference brought together industry leaders, researchers, and practitioners to showcase innovations, address critical challenges, and advance knowledge in geotechnical engineering. The conference hosted the Terzaghi, Peck, Seed, and Prakash Lectures and many technical sessions, panel sessions, short courses, and student competitions.

These proceedings represent the culmination of nearly two years of effort by the program committee and many other individuals, whose focus has been to continue the success of previous Geo-Congresses and to celebrate 30 years of geotechnical innovation by the Geo-Institute. Building the program started with an international call for papers that resulted in more than 800 abstracts on a variety of important topics. Each paper was subjected to a rigorous technical review by two or more independent peer reviewers. Acceptance required concurrence by at least two peer reviewers, and final decisions were made only after review coordinators confirmed that authors satisfactorily addressed any reviewer comments on their original submission. All accepted papers are presented at the conference as posters or technical talks and are eligible for applicable ASCE awards.

This volume contains a collection of 58 papers focused primarily on the topics of foundation engineering, earth retaining structures, and underground engineering and construction. This includes papers on deep foundations, soil-structure interaction, and numerical modeling of foundations and retaining wall systems.

The success of this conference and proceedings would not have been possible without the participation and collaboration of many individuals, including Brad Keelor, the tireless staff at the Geo-Institute, and the many session chairs and reviewers. We hope that these proceedings will be of use to the geotechnical engineering community for many years to come.

The Editors,

Jack Montgomery, Ph.D., P.E., M.ASCE, Auburn University
Brady R. Cox, Ph.D., P.E., M.ASCE, Utah State University

© ASCE

Acknowledgments

We are very grateful for the contributions of the authors, peer reviewers, session chairs, and program committee, without whom this publication would not be possible.

Geo-Congress 2026 Conference Program Committee

Conference Chairs
K. N. Gunalan, Ph.D., P.E., BC.GE, Pres. 20 ASCE, NAC, HNTB Corporation
Ryan B. Maw, P.E., G.E., BC.GE, F.ASCE, Gerhart Cole

Technical Chair
Shideh Dashti, Ph.D., M.ASCE, University of Colorado Boulder

Proceedings Editors
Brady R. Cox, Ph.D., P.E., M.ASCE, Utah State University
Jack Montgomery, Ph.D., P.E., M.ASCE, Auburn University

Student Program Liaison
Cassandra Rutherford, Ph.D., P.E., M.ASCE, Iowa State University

Program Committee Members
Aaron L. Leopold, P.E., M.ASCE, Dan Brown and Associates
Kam Ng, Ph.D., P.E., M.ASCE, University of Wyoming
Jenny Ramirez, Ph.D., P.E., M.ASCE, Geosyntec Consultants

© ASCE

Contents

Deep Foundations

A New, Multi-Scale Perspective on Polymer Support Fluids 1
Si Suo, Yongxin Wang, Stephan A. Jefferis, Martin J. Blunt, and Catherine O'Sullivan

Behaviour of Single Pile in Unsaturated Clay 7
Vinay Thakur and Ashutosh Kumar

Increase in Bridge Scour Causing Increase in Foundation Costs 18
Xinyi Jiang and Morgan Race

Centrifuge Modeling of Laterally Loaded Piles and CPT-Based *p–y* Curves in a Soft Clay 26
Shahriar Khorami, Mohammad Khosravi, Srikanth S. C. Madabhushi, and Ali Khosravi

Comparative Study of Under-Reamed and Conventional Piles Subjected to Horizontal Machine-Induced Vibration in Homogeneous Clay 36
Sayantan Banerjee and Debarghya Chakraborty

Consideration of Spatial Variability and Environmental Impacts in the Probabilistic Design of Driven Piles in Sand 47
Dora de Melo and Jason DeJong

Current Practice of Load and Resistance Factor Design of Driven Piles with Dynamic Testing and Analysis in the United States 58
Xiaoming Yang, Soonkie Nam, and Yuting Zhang

Disconnected Combined Pile-Raft Foundations: A Comprehensive Review for Optimal Performance 65
Arpita Ray and Deepankar Choudhury

These pages intentionally left blank 75

Effect of Soil Permeability of Liquefiable Ground on Pile Group Behavior: 3D Numerical Analysis 86
Sareh Kamran Jabbari, Morteza Rajabigol, and Fariborz M. Tehrani

Evaluating the Effect of General Scour on the Axial Capacity of Driven Piles Considering Pile Installation 95
Murad Y. Abu-Farsakh and Isam Khasib

© ASCE

Evaluating the Influence of Surface Characteristics on Shear Strength of Sand-Fines Mixture Soil-Foundation Interface 105
Mu'ath I. Abu Qamar, Azhar G. Hamad, Mohammad F. Tamimi, Ammar A. Alshannaq, and Aya A. Migdadi

Evaluation of End Bearing of Driven Steel H-Piles in Intermediate Geomaterials Based on Spherical Cavity Expansion Methods.....115
Nafis Masud, Kam Ng, and Shaun S. Wulff

Geotechnical Challenges and Innovative Solutions for the Hyundai Motor Group Metaplant America (HMGMA) in Georgia 128
Guoming Lin, Yan Jiang, Chao Zheng, and Morgan NeSmith

Improvement on Existing *p-y* Curves for Large-Diameter Piles in Cohesionless Soils.....140
Shin-Tower Wang, Jose Arrellaga, Luis Vasquez, and Daqing Xu

Large Diameter CFA-ACIP Piles in Laramie, Wyoming 151
W. Morgan NeSmith and Steven Duncan

Load Transfer in an End-Bearing Auger-Cast Pile: Laboratory-Scale Single-Pile Tests and Numerical Simulation 166
Edgar C. Correa-Prada, Jorge E. Orozco-Herrera, Jackson A. Gil-Hernandez, Sergio Marin-Savatier, Luis G. Arboleda-Monsalve, Kevin R. Mackie, and Rodrigo Herrera

Numerical Investigation of Micropile Group Lateral Capacity for Anchoring Floating Offshore Wind Turbines in Rocky Seabeds.....177
Neda Jamaleddin, Mohammed Gabr, Roy Borden, Richard Argall, and Donald Lasser

Numerical Simulation of Damage in Pile for Health Monitoring Using 3D-FEA 188
Sukanta Das, Satoshi Matsumura, Meisam Goudarzy, and Robert Kayen

Performance Evaluation of Deeply Embedded Ring Anchors in Saturated Sand.....199
Mohamed E. Ali, Junho Lee, and Charles Aubeny

Pore Pressure Accumulation and Pullout Capacity Reduction of Suction Anchor Foundations for Floating Offshore Wind Turbines under Cyclic Tensile Loading.....211
Amin Rafiei and Fahim Hassan

Predicting Axial Capacity of Pipe Piles Using Artificial Neural Networks.....220
Baturalp Ozturk, Antonio Kodsy, and Magued Iskander

© ASCE

Scenario-Based Field-Scale Evaluation of Thermal Performance of Ground Heat Exchangers **232**
Alireza Fakhrabadi, Aditya Deshmukh, Puneet Bhaskar, Xinbao Yu, and Anand J. Puppala

Strain Gauge Instrumentation of Spliced Concrete Piles in Soft Alluvial Soils **243**
Patrick A. Thurmond

Timber Piled Load Transfer Platform and GRS Abutments on Soft Ground for Temporary Panel Bridge **252**
Graham Elliott, Mark Landis, B. Philip Shull, and Kirsten Wilde Grant

Use of Expanded Polystyrene in Slab-on-Grade Concrete Foundation Systems for Thermal Insulation and Settlement Reduction **266**
Mahia Mahbub Riana, Jianxin Huang, Shanmukha Sai Avinash Gonnabathula, and Anand J. Puppala

Earth Retaining Structures

A Cofferdam Design with Finite Element Modeling Verification **276**
WenJun Dong and Yue Xu

Anchored Bridge Abutments and Soil Nail Walls in Upper Coastal Plain Soils: College Street Bridge, Macon, Georgia **287**
Graham Elliott, Justin T. Wood, and Ethan R. Brown

These pages intentionally left blank **301**

Case History of the Design of Temporary Earth Shoring in Clay Soil for the SLCIA TRP Central Tunnel **310**
Brian Garrett and Michael Haas

Case of Slope Collapse and Reinforcement of a Cut Retaining Wall Applied to the Colluvium Layer in the Limestone Zone **321**
Yong-Eun Roh, Min Ku You, and Ilhan Chang

Hybrid Surrogate Modeling of a Quay Wall: An Automatically Tuned Framework Integrating Long Short-Term Memory and Feedforward Neural Networks **332**
Kacper Cerek, Elnaz Hadjiloo, and Jürgen Grabe

In Situ Soil Stabilization and Support of Excavation Design for Remediation of a Former Manufactured Gas Plant **342**
Russell Lutch, Mac Bonner, Brandon Anderson, and Ricky Bradford

© ASCE

Incidence of Partial Failures in a Retention System Composed of Anchored Piles Using a Finite Element Model....356
Jackson A. Gil-Hernandez, Laura V. Rojas-Oviedo, Yerlin A. Astrudillo-Ramirez, and Luis G. Arboleda-Monsalve

Large-Scale Testing to Evaluate Lightweight Cellular Concrete Backfill behind MSE and Cantilever Walls 366
Kyle M. Rollins, Ryan B. Maw, Ryan J. Wilkinson, Christian Lundskog, Meghann Morgan, and Mathew R. Bueckers

Numerical Analysis of Horizontal Obstruction Failures under MSE Walls 381
Md. Asad Ahmad and Antonio Bobet

Numerical Study of MSE Wall Performance as Bridge Foundation 392
Adams Familusi, Ahmed Abu El Ela, Yunesh Saulick, Vincent Ogunro, and John Daniels

Post-Failure Stability Analyses of I-295, Wall 22 401
Alexander Reeb and George Filz

Retaining Wall Deformation Monitoring with Camera Array Systems....417
Qingyu Ren, Hui Wang, and Sreelakshmi Sreeharan

Seismic Active Lateral Earth Pressure on Retaining Walls with Broken Slope Backfill: A Finite Element Limit Analysis Approach 427
Ali Shafiee and Amir Hossein Shafiee

Seismic Stability of Reinforced Soil Wall: A Modified Pseudo-Dynamic Approach 436
Sushree Paritwesha Pradhan and Vishwas A. Sawant

Underpinning and Earth Retention for Temple Square Renovation in Salt Lake City, Utah 446
Rob Jameson, Eric Lindquist, Scott Chambers, Josh Fenn, and Taylor Nordquist

Shallow Foundations

Reliability Analysis for Differential Settlement of Shallow Bridge Foundations in Cohesionless Soils....462
Aseel Y. Ahmed, Andrzej S. Nowak, and Brian T. Havens

Underground Engineering and Construction

Advanced Ground Settlement Monitoring in Urban Excavation Using Multi-Sensor UGV Technology 471
Young-Hoon Jung, Taesik Kim, Jinman Jung, and Hong Min

© ASCE

Cottonwoods Connection Pipeline Crossing of the Wasatch Fault 480
Travis Gerber and Ryan Maw

Cut-and-Cover Construction Using Floating Diaphragm Walls—A Case Study.....490
Chu E. Ho

Dual-Auger Bio-Inspired Self-Burrowing Robot (BurroBot): Laboratory Evaluation of Horizontal Burrowing Behavior 503
Sarina Shahhosseini and Junliang (Julian) Tao

Evaluation of Bearing Capacity for TBM Tunneling in Deep Soft Soils 513
Chu E. Ho and Vishnu Saketh Jella

Feasibility Study on Health Monitoring of Buried Structures Using Battery-Free and Cable-Free Sensors 524
Jun Wang, Fei Wang, Yu Luo, Lina Pu, Isaac L. Howard, and William Crook

GIS Interoperability Framework for Risk Management in Tunneling Projects 535
Rajat Gangrade and Steve Savage

Groundwater Control and Excavation Support for the Salt Lake City Water Reclamation Facility Influent Pump Station 543
Scott Chambers, Eric Lindquist, and Scott Simmons

Impact of Arch Geometry on Subsurface Settlement Prediction due to Tunnelling in Sand Considering Soil Arching 552
Venkata Ramana Medishetty, Quamar Tabish, and Kousik Deb

Impact of Grout Strength on Performance of Rehabilitation Corroded Steel Pipes under Parallel-Plate Loading Tests.....564
S. Mustapha Rahmaninezhad, Jie Han, and Robert L. Parsons

Influence of Boundary Conditions on Centrifuge Tunnel Tests.....573
Felipe P. M. Vitali, Osvaldo P. M. Vitali, Tarcisio B. Celestino, and Antonio Bobet

Innovative InSAR-Based Method for Multi-Scale Risk Assessment of Seasonal Impacts on Water Main Breaks.....581
Yusheng Jiang, Hui (Jack) Wang, and Xiong (Bill) Yu

Laboratory Investigation on Advancing an Eco-Friendly Backfill Grout for Shield TBM Tunneling Using Biopolymer-Based Soil Treatment (BPST) 591
Hyungbin Park, Chanjo Kwon, and Ilhan Chang

© ASCE

Numerical Modeling of Centrifuge Tunnel Tests Using the NorSand and Hardening Soil Models 601
Felipe P. M. Vitali, Ricardo C. Formigari, and Osvaldo P. M. Vitali

Performance-Based Testing of Trenchless Pipeline Rehabilitation 610
Sina G. Senji, Brad P. Wham, and Shideh Dashti

© ASCE

A New, Multi-Scale Perspective on Polymer Support Fluids

Si Suo, Ph.D.[1]; Yongxin Wang, Ph.D.[2]; Stephan A. Jefferis, Ph.D.[3]; Martin J. Blunt, Ph.D.[4]; and Catherine O'Sullivan, Ph.D.[5]

[1]Researcher, Dept. of Civil and Environmental Engineering, Imperial College London, London, UK. Email: s.suo@imperial.ac.uk
[2]Dept. of Civil and Environmental Engineering, Imperial College London, London, UK. Email: yongxin.wang22@imperial.ac.uk
[3]Environmental Geotechnics Ltd., Banbury, UK. Email: envgeot@gmail.com
[4]Professor, Dept. of Earth Science and Engineering, Imperial College London, London, UK. Email: m.blunt@imperial.ac.uk
[5]Professor, Dept. of Civil and Environmental Engineering, Imperial College London, London, UK (corresponding author). Email: cath.osullivan@imperial.ac.uk

ABSTRACT

Polymer fluids have emerged as promising alternatives to bentonite-based slurries in excavation support applications for piles and diaphragm walls. However, their flow behavior and mechanical interaction with soil grains remain insufficiently understood. This paper presents a multiscale numerical framework based on pore-network modeling (PNM) to investigate non-Newtonian polymer flow in porous media and its implications for excavation support. A customized PNM approach is developed to simulate flow patterns, flow heterogeneity, and grain drag forces in sphere packings representing sandy soils. The results reveal three distinct flow regimes. A non-linear drag-pressure gradient relationship above a critical threshold is predicted, and the implications for safety factors in design are discussed. The framework is extended to a field-scale penetration model using a generalized Darcy's law, capturing the transition in polymer penetration dynamics over time. The findings provide valuable insights for the design and assessment of polymer fluid-supported excavations.

INTRODUCTION

Polymer fluids, i.e., aqueous solutions containing long-chain polymers, have gained increasing attention in geotechnical engineering due to their potential as effective alternatives to bentonite-based slurries in excavation support applications. These fluids offer several practical advantages, including reduced environmental impact, easier disposal, and compatibility with a variety of soil types (Lam and Jefferis 2018). However, despite their growing usage, a fundamental understanding of polymer fluid behavior in porous geomaterials remains limited, hindering their broader adoption in engineering practice. Especially for sandy and permeable soils, there is uncertainty around the support forces imparted to the soil.

The complexities stem primarily from the non-Newtonian nature of polymer fluids. Unlike water or other Newtonian fluids which have constant viscosity, polymer fluids typically exhibit shear-thinning rheology, i.e., their apparent viscosity decreases with the shear rate (Lam et al. 2015). This characteristic introduces significant nonlinearities in fluid behavior at the pore scale, making it challenging to predict flow distributions and associated mechanical effects such as drag forces exerted on soil grains. These grain-scale interactions play a critical role in determining the stability and performance of excavation support systems using polymer fluids.

© ASCE

In response to this challenge, this study provides a multiscale perspective, as illustrated in Figure 1, by synthesizing recent advances in pore-scale modeling of non-Newtonian fluid flow in porous media and upscaling techniques. The goal of this paper is to integrate these modeling efforts into a coherent package that spans fundamental modeling, pore-scale analysis, and engineering application. By linking polymer fluid rheology to grain-scale drag and macro-scale support behavior, this work contributes both to the state of the art in non-Newtonian flow modeling and to geotechnical engineering design.

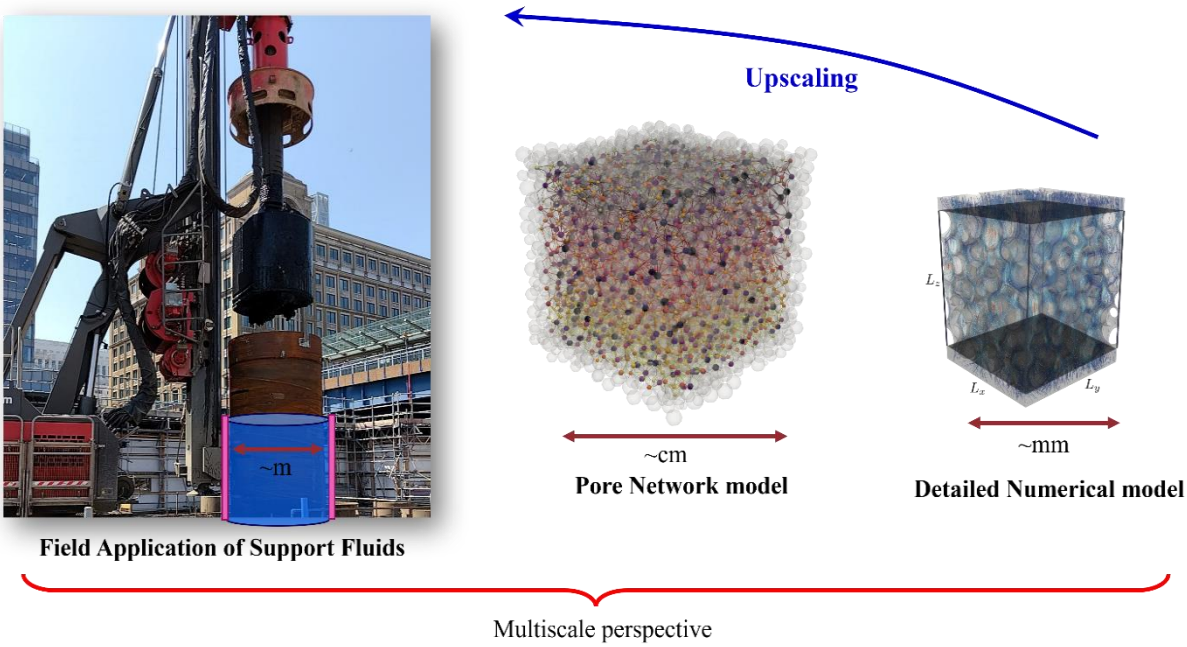


Figure 1. A schematic illustrating the multiscale nature of this work.

Modeling and Results

Pore-network model

Pore network modeling has emerged as a computationally efficient technique to simulate flows in porous media including soil (Blunt et al. 2013; Chareyre et al. 2012; Morimoto et al. 2024). In a pore network model the nodes are the voids or pores and the edges are the pore throats that connect the pores. Each edge (throat) is assigned a fluid conductance that depends on the throat morphology. Using these conductance values and knowing the note connectivities a system of equations can be created and solved to obtain the flow in individual throats. The process is very similar to a pipe network analysis that is used to obtain the flow in individual pipes in an urban water distribution network.

The key challenge is to obtain conductances in the case of the non-Newtonian polymer fluids considered here. We developed a conductance model (flow-pressure gradient relationship) for individual pore throats (network edges) using the power-law model to simulate the fluid polymer rheology shown in Figure 2(a). This model was then integrated into a customized pore-network modeling (PNM) framework that captures both the complex fluid rheology and the geometry of granular media (Suo et al. 2025).

© ASCE

In this study, model porous media comprising sphere packings were created representing a wide range of sandy soils by adjusting particle size distribution and porosity, as shown in Figure 2(b). The corresponding pore networks are extracted based on the image segmentation and the maximal-ball algorithm for network extraction (Dong and Blunt 2009). Once this network of pores and throats has been extracted, flow of polymer fluids through the system was simulated.

Our PNM simulations reveal three key features of polymer fluid flow in porous media:

1. Three flow regimes are identified as shown in Figure 2(c), i.e., the Darcy regime at low pressure gradient ($|\nabla P|$) in which $|q| \propto |\nabla P|$ (where q is the flow rate), the power-law regime at high $|\nabla P|$ in which $|q| \propto |\nabla P|^{1/n}$, and a transition regime to bridges these two limiting regimes.
2. At the micro-scale, the shear-thinning rheology enhances the flow heterogeneity and preferential pathways form through the larger, faster-flowing portions of the pore space in the power-law regime.
3. At macro-scale, the flow can be described using a generalized Darcy's law. This was validated against permeameter test data (Ejezie et al. 2021), paving the way for the following field-scale modeling.

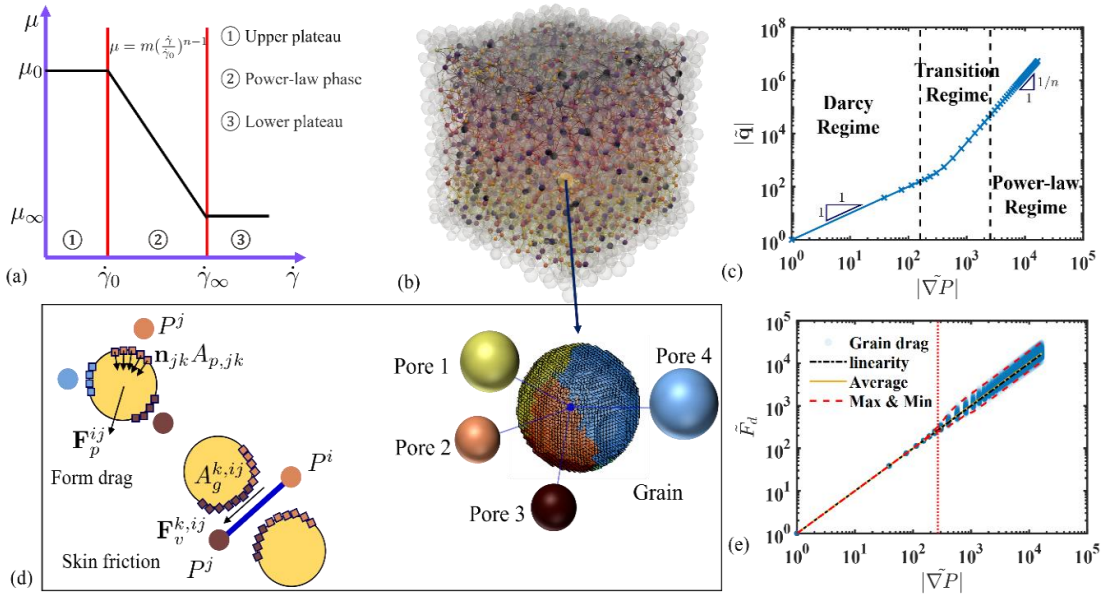


Figure 2. (a) (b) The power law model for characterizing the rheology of polymer fluids. (b) Pore network extracted from sand packing. (c) Evolution of Darcy velocity $|q|$ with pressure gradient $|\nabla P|$ for the three flow regimes, i.e., Darcy regime, transition regime, and power-law regime. (d) Zoom-in plot of schematic of the grain-pore interface. (e) Normalized drag force $\widetilde{F}_d$ of all complete grains in the packing at different $|\nabla P|$.

Drag force

From the flow and pressure data available from the PNM, the fluid-grain interaction force was calculated by considering its two components, i.e., the form drag arising from the fluid pressure normal to the grain and the skin friction induced by the viscous shear along the grain surface. As schematically illustrated in Figure 2(d), the form drag is calculated as a summation

© ASCE

of the pore pressure force from a grain's neighboring pores; the skin friction is calculated using the method proposed in Chareyre et al. (2012). This calculation module of grain drag was validated against a small-scale high resolution flow simulations (direct numerical simulation) using the open-source CFD code OpenFOAM v2106.

By employing this modeling technique, we numerically investigate grain drag induced by polymer fluid flow in sands. The numerical results reveal a unique phenomenon that the shear-thinning rheology enhances the flow heterogeneity. Consequently, there exists a critical threshold pressure gradient $|\nabla P|_t$ beyond which the grain drag no longer scales linearly with pressure gradient $|\nabla P|$, as shown in Figure 2(e). The critical pressure gradient $|\nabla P|_t$ depends on both fluid rheology and intrinsic permeability.

This nonlinear drag response may cause uncertainties in engineering. When $|\nabla P| > |\nabla P|_t$, the normalized grain drag varies between grains, suggesting that some grains experience elevated drag, beneficial to excavation support, while others may receive insufficient drags, posing stability risks. Therefore, to guarantee excavation design, a safety factor should be applied on the total support force when $|\nabla P| > |\nabla P|_t$. This factor can be defined using a 95% confidence level ensuring 95% grains have sufficient drag. Simulations across various sand samples indicate the safety factor in the range of 0.7 to 0.9.

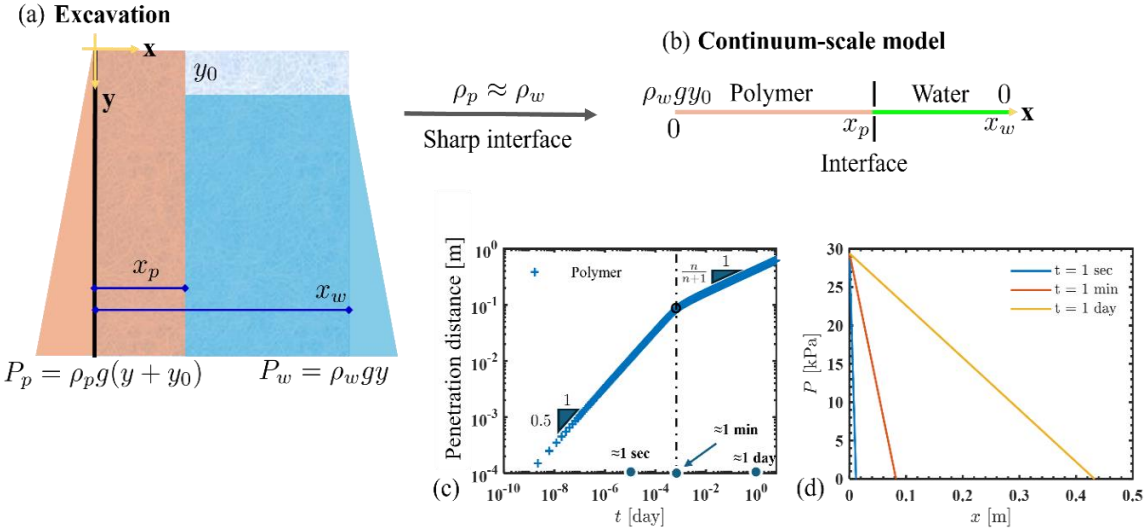


Figure 3. (a) Schematic of an excavation with polymer permeating the adjacent soil and (b) its corresponding 1D continuum-scale model. (c) Dynamics of penetration distance and (d) pressure distribution.

Field-scale modeling

Figure 3(a) depicts a planar model representing a long trench excavation. In this model, the polymer support fluid (in orange) is driven to displace the underground water (in blue) in a soil layer by a constant polymer head greater than the water table. The difference in density of water and polymer solution is less than 0.2% allowing us to assume equal densities. The interface between the two fluids is assumed to be vertical and sharp, since the displacement is viscously stable. Based on these two assumptions, the problem can be simplified as a one-dimensional model as shown in Figure 3(b). In the polymer-saturated phase, the flow is described using the

© ASCE

proposed generalized Darcy's law while the classical linear Darcy law is used in the water-saturated phase. Furthermore, because the apparent viscosity of polymer fluids is much larger than that of water, pressure drop occurs almost entirely across the polymer phase, which leads to a conservative, upper-limit estimate of penetration dynamics.

As an example, we consider a soil with hydraulic conductivity of 10^{-4} m/s and porosity of 0.32 permeated by the polymer solution of 1.0 kg/m^3 concentration. The parameters involved are listed in Table 1. As shown in Figure 3(c), polymer penetration occurs in two distinct phases. In the very beginning, the polymer penetrates faster, i.e., the penetration distance is proportional to $t^{0.5}$, due to the dominance of the lower plateau viscosity. After a very short period (around 1 minute), the pressure gradient diminishes and power-law viscosity dominates, slowing penetration, i.e., the penetration distance is proportional to $t^{\frac{n}{n+1}}$. This pressure gradient reduction is clearly illustrated in Figure 3(d).

Table 1. Model parameters used in Figure 3

Parameter		Value
Soil	Soil porosity	0.32
	Hydraulic conductivity (m/s)	10^{-4}
	Head difference between polymer and water (m)	3
Polymer fluid	Lower plateau viscosity (Pa s)	10
	Upper plateau viscosity (Pa s)	3
	Power law index n	0.26
	Scaling coefficient m (Pa s)	0.73

CONCLUSION

By employing pore-network modeling and high resolution simulation of flow in the pore space of a model soil, we have shown that a micro-macro analysis approach can address a practical geotechnical design challenge by providing new insight into the mechanics of polymer fluid support systems and contributing both to theoretical understanding and engineering practice in excavation support design. We have shown that these models can be used to address real challenges encountered in the field, i.e. polymer loss estimation and excavation stability analysis.

ACKNOWLEDGMENTS

This work was funded by the EPSRC grant EP/X034305/1: Permeation of polymer fluids in soils (PoPFS) and the UKRI Access to HPC call APP36940 (ARCHER2): Modelling permeation of polymer support fluids in soils using a combined CFD and DEM approach. We acknowledge the discussions with Prof. Chris MacMinn and Dr. Callum Cuttle at University of Oxford, Dr. Brian Sheil and Dr. Marina Bortolotto at University of Cambridge, and Mr. Chris Barker at Arup.

REFERENCES

Blunt, M. J., Bijeljic, B., Dong, H., Gharbi, O., Iglauer, S., Mostaghimi, P., Paluszny, A., and Pentland, C. (2013). "Pore-scale imaging and modelling." *Advances in Water Resources*, 51, 197-216.

© ASCE

Chareyre, B., Cortis, A., Catalano, E., and Barthélemy, E. (2012). "Pore-Scale Modeling of Viscous Flow and Induced Forces in Dense Sphere Packings." *Transport in Porous Media*, 94(2), 595-615.

Dong, H., and Blunt, M. J. (2009). "Pore-network extraction from micro-computerized-tomography images." *Physical Review E*, 80(3).

Ejezie, J. O., Jefferis, S. A., Lam, C., Sedighi, M., and Ahmad, S. M. (2021). "Permeation behaviour of PHPA polymer fluids in sand." *Géotechnique*, 71(7), 561-570.

Lam, C., and Jefferis, S. A. (2018). *Polymer support fluids in civil engineering*, ICE Publishing London.

Lam, C., Martin, P. J., and Jefferis, S. A. (2015). "Rheological properties of PHPA polymer support fluids." *Journal of Materials in Civil Engineering*, 27(11), 04015021.

Morimoto, T., O'Sullivan, C., and Taborda, D. M. G. (2024). "Applying Network Modeling to Determine Seepage-Induced Forces on Soil Particles." *Journal of Geotechnical and Geoenvironmental Engineering*, 150(5).

Suo, S., Foroughi, S., Blunt, M. J., and O'Sullivan, C. (2025). "Pore-network modeling of polymer flow in porous media." *Computers and Geotechnics*, 182, 107142.

© ASCE

Behaviour of Single Pile in Unsaturated Clay

Vinay Thakur[1] and Ashutosh Kumar, Ph.D.[2]

[1]Ph.D. Research Scholar, School of Engineering, IIT Mandi, Himachal Pradesh, India (corresponding author). Email: d23121@students.iitmandi.ac.in
[2]Assistant Professor, School of Engineering, IIT Mandi, Himachal Pradesh, India. Email: ashutosh@iitmandi.ac.in

ABSTRACT

This study presents the results of numerical modelling to investigate the behaviour of a single pile foundation embedded in an unsaturated clay. A finite element-based program Abaqus was used to develop a 2D axisymmetric soil pile model, and the simulations were performed using the finite element code numgeo. The pile was modelled as linear elastic and the soil as elastic-perfectly plastic using the Mohr-Coulomb model extended with Bishop's effective stress, having parameters calibrated using laboratory testing. The hydromechanical behaviour of soil was incorporated using van Genuchten model. The static steady-state analysis was carried out to understand the pile response under different suction profiles obtained using laboratory measured data. After successful validation of the development numerical model using physical testing results, parametric study was also carried out by varying pile geometry. The obtained results revealed that pile capacity increased significantly as suction in soil increased from 0 kPa to 1,716 kPa. However, as soil entered the residual zone of unsaturation, the contribution of suction toward the increase in capacity decreased significantly. Additionally, the parametric study on pile geometry highlighted a substantial increase in the load carrying capacity as slenderness ratio decreased from 62 to 31 across all suction ranges.

Keywords: Pile foundation, unsaturated clay, finite element method, suction

INTRODUCTION

The load transfer mechanism in pile foundations is primarily governed by the interaction between the pile shaft and the surrounding soil. Numerous studies have investigated soil–pile interaction, emphasizing that the load–settlement response of pile foundation is highly dependent on the stiffness and shear strength of the surrounding soil (Poulos 1989). These studies assumed soil to be either fully saturated or completely dry, overlooking the real case scenarios of partial saturation in the vadose zone above the water table (Al-Khazaali and Vanapalli 2019). These conditions are especially prevalent in arid and semi-arid regions which constitute over 49% of the Earth land area (Achten et al. 2013). In these areas, the suction stresses enhance effective stresses, thereby improving both the shear strength and stiffness of the soil (Vanapalli et al. 1996; Oh et al. 2009; Oh and Vanapalli 2013). These suction-induced shear strength improvements significantly affect soil-pile interaction thereby influencing the load-settlement response of the pile foundations (Kumar and Kumar 2023a).

Recognizing this, several researchers conducted model pile load testing demonstrating that suction stresses within the soil matrix enhance soil stiffness and shear strength (Vanapalli et al. 2010; Sheikhtaheri 2014; Liu and Vanapalli 2022). Centrifuge testing conducted by Lee and Lee

© ASCE

(2025) revealed that variations in the groundwater table along the pile depth can substantially alter suction stress distribution at the pile–soil interface, thereby impacting the load-carrying capacity of pile foundations and therefore neglecting these effects can lead to overly conservative and uneconomical foundation design. To incorporate suction effect in pile design, Vanapalli and Taylan (2011;2012) modified the conventional α, β and λ method to extend their applicability to unsaturated soil conditions. Pham et al. (2024) proposed a simplified analytical approach to capture the development of non-linear interface shear stresses with respect to change in suction. Georgiadis et al. (2003) conducted early numerical analyses on pile foundations in unsaturated soils, demonstrating the influence of rise in groundwater table on pile capacity. Building on this, more advanced studies by Han et al. (2016); Wu and Vanapali (2022); Kumar and Kumar (2023b;2023c) implemented Soil Water Retention Curve (SWRC) parameters into numerical simulations to account for change in suction with respect to drying and wetting of soil profile and its effect on the load mobilization mechanism of a single pile. While existing studies emphasized the need to accurately represent suction stresses for realistic simulation of pile behaviour in unsaturated soils, many did not account for the full range of suction variations during wetting and drying cycles. Moreover, research on coupled hydromechanical response in unsaturated low-plasticity clays remains limited in current literature.

This paper presents the results of numerical investigation that had been carried out on single pile foundation embedded in unsaturated low-plastic clay. The study employed a static steady state analysis to simulate the hydro-mechanical response of the pile-soil system using finite element code numgeo. The developed numerical model was subjected to a range of matric suction values which has been observed during the drying cycle of the soil in laboratory experiment to account for the suction-dependent stiffness variation. Additionally, the study also investigated the effect of varying slenderness ratio on the load–settlement behaviour of pile foundation embedded in unsaturated soil conditions.

DEVELOPMENT OF NUMERICAL MODEL AND VALIDATION

The two-dimensional axisymmetric finite element model employed in present study was developed to closely replicate the 1-g physical laboratory model used in experimental investigation carried out by Kumar et al. (2025). The physical model consisted of a soil tank with dimensions 580 mm × 580 mm × 900 mm and the tank was filled with soil to a depth of 820 mm. A closed-ended aluminium pile with a diameter of 12 mm and total length of 700 mm was installed vertically at the geometric centre of the tank using the wished-in-place installation method with final embedded depth of 620 mm as shown in Figure 1(a). The physical model was specifically designed and instrumented to enable comprehensive of monitoring the water migration, suction variation and resulting deformation in the pile foundation.

To simulate the load-settlement behaviour, a simplified axisymmetric geometry was adopted. The model geometry was created using the finite element software Abaqus 2022 and the axisymmetric model consisted of a soil domain with width 290 mm and depth 820 mm and a model pile embedded within the soil as illustrated in Figure 1(b). The developed model geometry was then extracted from the Abaqus and exported to the finite element program *numgeo* for simulation. *numgeo* is an advanced finite element code capable of addressing non-linear, coupled and dynamic geotechnical problems (Machacek and Staubach 2021). In this code, a single phase non-porous axisymmetric solid elements u4-solid-ax with 4 nodes were assigned to the pile geometry and a linear elasticity model was implemented to model the pile response. A coupled

© ASCE

pore pressure-displacement elements u4p4-stab-ax-red with 4 nodes were assigned to the soil domain. These elements are three-phase porous solid elements which follow the theory of porous media and Taylor-Hood formulation to simulate the solid-fluid fully coupled materials response. An elastic-perfectly plastic Mohr-Coulomb model was incorporated to model the mechanical behaviour of unsaturated low plasticity clay by extending the constitutive model application using the concept of Bishop's effective stress to consider the effect of suction stresses on the shear strength of soil as per Equation 1 and 2 (Bishop 1959; Bishop and Blight 1963):

$$\sigma'_{ij} = \sigma_{ij} - p^a 1_{ij} + \chi(p^a - p^w)1_{ij} \quad (1)$$

$$\tau = c'1_{ij} + \left(\sigma_{ij} - p^a 1_{ij}\right)tan\phi' + \chi(p^a - p^w)1_{ij}tan\phi' \quad (2)$$

Where σ'_{ij}= effective stress; σ_{ij}= total stress; X= averaging parameter assumed as effective degree of saturation; $(p^a - p^w)$= suction; τ = Shear strength of soil; c'= effective cohesion; and ϕ'= effective angle of shearing resistance. van Genuchten (VG) model (1980) was used to model the hydro-mechanical response of the soil.

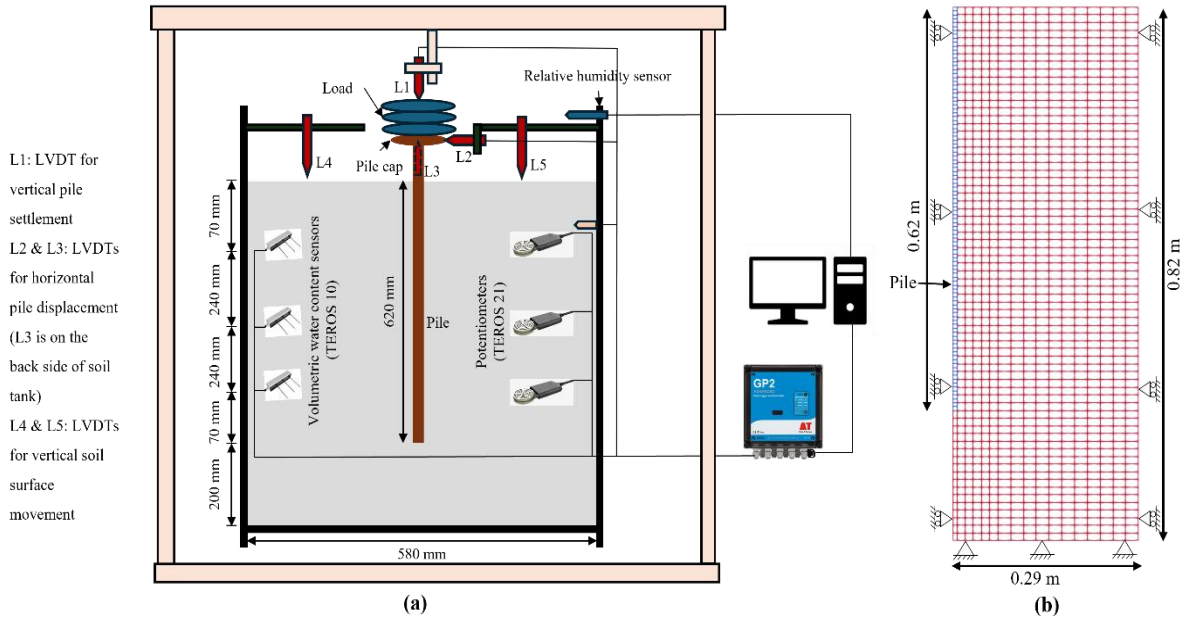


Figure 1. (a) 1g laboratory scale physical model (Adopted from Kumar et al. 2025) (b) Two-dimensional axisymmetric soil pile model

Table 2 summarizes the model parameters for unsaturated clay, where the shear strength was defined using critical state parameters. This approach is widely adopted in geotechnical modelling, as soil behaviour at large strains tends to converge to the critical state and adopting the critical state friction angle ensures consistency with Bishop's effective stress framework (Wheeler et al., 2003). The mechanical boundary conditions were assigned in such a way that the base of model tank was restrained in all the direction and sides were restricted in lateral directions. To simulate the soil-pile interface, the penalty approach was used and contact constraints were enforced assuming no separation condition between soil-pile interface. A

© ASCE

Coulomb interface friction model was implemented to model the frictional contact between the soil and pile. The value of wall friction angle coefficient was provided as 0.38 as per IS 2911, Part 4 (BIS 2013). A mesh sensitivity analysis was conducted to evaluate the influence of mesh density on the simulation results. Based on this, the soil was discretized using 4-noded stabilized linear axisymmetric three phase porous solid element. This element is specifically designed for hydromechanical analyses and its reduced integration scheme improves computational efficiency while maintaining numerical accuracy.

A systematic calibration of constitutive model parameters was undertaken to accurately simulate the mechanical response of low plasticity clay. Experimental results of oedometer and consolidated undrained triaxial tests were used to identify the input parameters for the Mohr–Coulomb model. The element tests were simulated in *numgeo* using axisymmetric solid elements, and multiple iterations were performed to refine the parameters. Through this iterative calibration process, the numerical results achieved close agreement with the experimental observations, confirming the reliability of the model in capturing the response of clay. The calibrated parameters are mentioned Table 1.

Table 1. Mechanical and hydraulic model parameters for low plasticity clay

Mohr-Coulomb model parameters				
Poisson's ratio μ	Saturated Young's modulus (kPa)	Cohesion (kPa)	Critical angle of shearing resistance ϕ_c (°)	Dilation angle Ψ (°)
0.35	5900	0	31.5	0
VG model parameters				
Residual degree of saturation (S^{wr})	α (m^{-1})		n	
0.2	0.025		1.7	

To capture the influence of suction on soil stiffness, the Vanapalli-Oh model (Equation 3 and 4) was incorporated and unsaturated modulus of elasticity was calculated for different suction levels (Vanapalli and Oh 2010).

$$E_{unsat} = E_{sat}\left[1 + \frac{\alpha(u_a - u_w)}{\left({}^{P_a}/_{100}\right)} S^{\beta}\right] \tag{3}$$

$$\frac{1}{\alpha} = 0.5 + 0.312\left(I_p\right) + 0.109\left(I_p\right)^2 \tag{4}$$

Where, E_{unsat} = unsaturated modulus of elasticity, E_{sat} = saturated modulus of elasticity, $(u_a - u_w)$ = matric suction, P_a = 101.3 kPa is atmospheric pressure, S = degree of saturation, α and β are fitting parameters where α = 0.114 calculated using Equation 4 and β = 2.

The static steady state analysis of unsaturated soils requires incorporating the hydromechanical behaviour of soil. To accurately simulate the pile response under drying conditions, the van Genuchten (VG) model (van Genuchten 1980) was incorporated using the soil-water retention curve (SWRC) parameters corresponding to the drying phase of the unsaturated clay. These parameters were obtained by curve-fitting drying-phase SWRC data reported by Kumar et al. (2025) as shown in Figure 2. Equation 5 and 6 proposed by van

© ASCE

Genuchten (1980) were used in *numgeo* to define the relationship between soil suction and degree of saturation.

$$S^e = \left(\frac{1}{1+(\alpha s)^n}\right)^{1-1/n} \quad (5)$$

$$S^w = S^{wr} + (1 - S^{wr})\left(\frac{1}{1+(\alpha s)^n}\right)^{1-1/n} \quad (6)$$

Where, S^e = effective degree of saturation; s = suction (kPa); α and n are the empirical curve-fitting parameters; S^w = degree of saturation, S^{wr} = residual degree of saturation. The fitted air entry value was reported as 400 kPa and the VG model parameters are presented in Table 1.

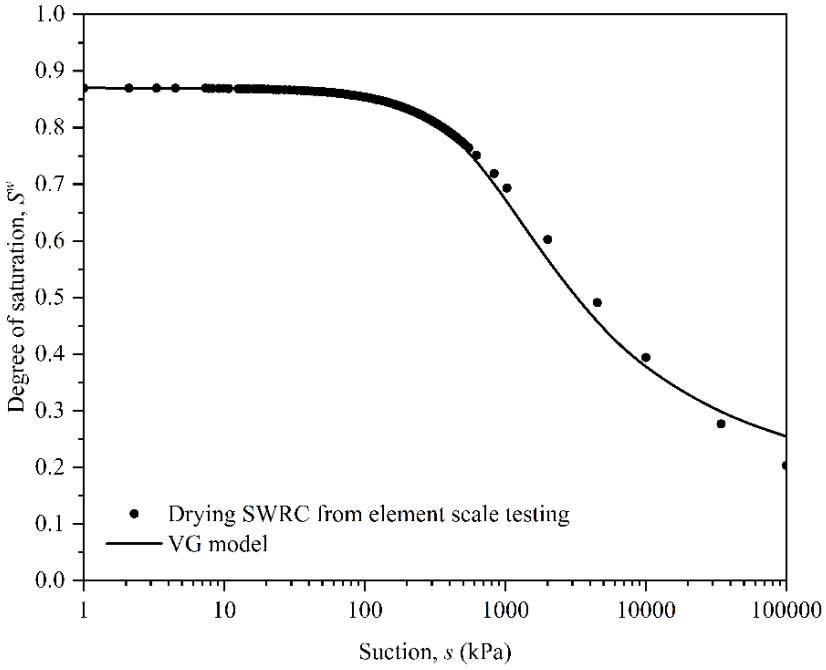


Figure 2. Drying Soil-water retention curve of low plasticity clay and Curve fitting using vG model (Re-drawn after Kumar et al. 2025)

The developed numerical model was validated with the load-settlement response of 1g physical model. The model was initialised such that the initial conditions of the physical model was replicated. A uniform value of suction (u_a-u_w = 28 kPa) was provided. The corresponding unsaturated modulus of elasticity was calculated using Equation 3. The initial state of stresses in the soil was generated using the standard K_o procedure. The *numgeo* code required the permeability of solids value which was calculated using the procedure given in *numgeo* manual and calculated value is reported in Table 2. Thereafter, a vertical ramp loading of 192 N was applied on to the pile head along the axis of symmetry of single pile and load-settlement response was simulated. The simulation results predicted a pile settlement of 0.46 mm, closely matching the experimental value of 0.45 mm under the same loading conditions. The obtained load-settlement response was also showed a good agreement with the 1g physical model test

© ASCE

results indicating the validation of the developed numerical model as shown in Figure 3(a). The corresponding strain contours was shown in Figure 3(b) demonstrating the soil deformation observed in the model at the end of the loading. The input material parameters for clay and pile are presented in Table 2.

Table 2. Input material parameters for soil and pile used in simulation

Parameters	Soil						Pile
Suction (u_a-u_w) (kPa)	0	28	389	893	1211	1716	-
Modulus of elasticity E (kPa)	5900	20170	34520	49110	63275	72946	21,000,000
Unit weight γ (kN/m^3)	19.52						78
Poisson's ratio (μ)	0.473						0.3
Critical angle of shearing resistance ϕ_c (°)	31.5						-
Dilation angle ψ (°)	0						-
Cohesion c (kPa)	0.00						-
Plasticity index (I_p)	7.43						-
Permeability of solids (m^2)	2.097×10^{-16}						-

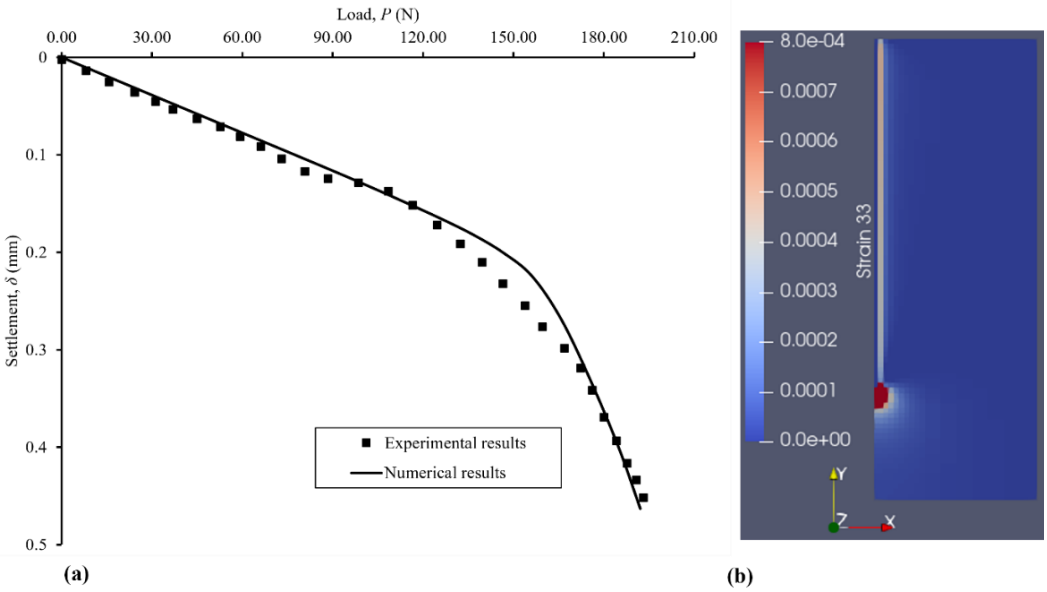


Figure 3. (a) Load-settlement response of single pile obtained using numerical analysis and physical modelling, (b) Stain contour obtain after the application of 192 N load

© ASCE

RESULTS AND DISCUSSION

Load-settlement response under varying suction

To simulate the hydromechanical behaviour of pile foundations embedded in unsaturated clay, the developed soil pile model was subjected to wide ranges of matric suction to replicate the drying conditions observed in the physical laboratory setup. The unsaturated soil was exposed to a prolonged drying period of 205 days in the laboratory experiment during which suction developed progressively. Based on the temporal variation in suction, average matric suction values 28 kPa, 389 kPa, 893 kPa, 1211 kPa and 1716 kPa corresponding to day 1, 50, 100, 150, and 200 were applied in the numerical model to replicate the physical model conditions. Consequently, an incremental mechanical loading was applied on to the pile top and load-settlement response was simulated.

Figure 4(a) shows the load-settlement response of a single pile with *l/d* ratio of 51.7 embedded in unsaturated low-plasticity clay subjected to varying suction values. The results clearly demonstrated a substantial increase in the load-carrying capacity of pile with increase in suction levels. Pile capacity increased by 368% as suction increased from 0 to 28 kPa and as suction further increased from 28 kPa to 1716 kPa, the load–settlement response of the pile exhibited a consistent and significant improvement. This is mainly because suction enhances shear strength and stiffness in soil by promoting interparticle bonding and friction through capillary water menisci, thereby improving soil-pile interaction (Vanapalli et al. 1996). However, beyond 1211 kPa suction which corresponds to the residual zone of unsaturation in clays, a marginal increase of 15% in pile capacity was observed indicating limited increase for higher suction ranges. This observed behaviour was consistent with the findings of Vanapalli et al. (1996) who reported that as fine grain soils enters the residual zone of saturation (typically greater than 1500 kPa), the suction increase no longer contributes significantly to effective stress due to the breakdown of capillary water menisci between soil particles, which are the primary mechanism for suction-induced strength in unsaturated soils.

Figure 4(b) shows the results of ultimate capacity (P_{ult}) of model pile with respect to suction (s). The P_{ult} of pile was calculated using the double-tangent method suggested by Butler and Hoy (1997). The method involves plotting the load-settlement response and drawing two tangents, one to the initial linear portion of the curve and second with plastic portion of the curve to represent the failure phase as shown in Figure 4(a). The intersection point of these two tangents defines the ultimate capacity of pile foundation. The obtained results clearly demonstrated that increase in soil suction led to significant increase in the ultimate capacity of the model pile, especially at lower suction levels. An initial increase in suction from 0 kPa to 28 kPa resulted in a substantial 590% increase in ultimate capacity. However, as suction further increased to 1716 kPa, the rate of increase in capacity reduced progressively indicated by the decreasing slope of P_{ult} with respect to s curve. The reduction was particularly significant from 1211 kPa to 1716 kPa where increase in P_{ult} value was limited to only 15%. The observed behaviour was consistent with the study of Nishimura et al. (2008) and Vanapalli and Oh (2010) which describe the dependency of soil stiffness on the suction and degree of saturation. As soil suction increases, the corresponding degree of saturation decreases and in case the residual suction zone, the incremental gains in stiffness and strength become negligible as degree of saturation corresponding to the suction value is very small. Therefore, under near-dry conditions, the additional contribution of suction to soil strength and stiffness is limited. As a result, the

© ASCE

influence of suction on soil-pile interaction weakens, thereby limiting further improvements in the load-carrying capacity of pile foundations in unsaturated clays.

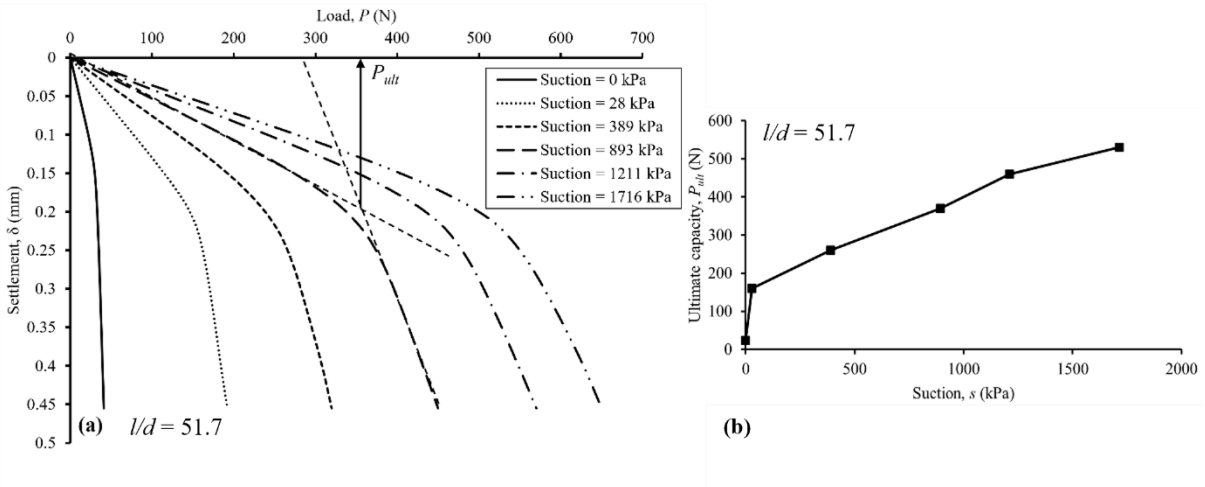


Figure 4. (a) Load settlement response of single pile under different average suction values (b) Ultimate capacity of model pile with respect to suction

Effect of slenderness ratio on load-settlement response for pile

To evaluate the influence of pile geometry on load-settlement response, a series of numerical analyses were performed by varying the slenderness (*l/d*) ratio. The pile length was kept constant at 620 mm, while the diameters were varied as 10 mm, 12 mm, 14 mm, 16 mm, 18 mm, and 20 mm, corresponding to *l/d* ratios of 62, 51.7, 44.3, 38.7, 34.4, and 31, respectively.

Figure 5(a) presents the load settlement response of single pile with different *l/d* ratio embedded in soil at 389 kPa suction. The results clearly demonstrated that load-carrying capacity of pile increased with decrease in *l/d* ratio. As the *l/d* ratio reduced from 62 to 31, the pile capacity increased by 85% and most significant increase of 23% was observed when the ratio was reduced from 62 to 51.7. However, further reduction in *l/d* ratio below 34.44, resulted in only a 4.5% increase in pile capacity, indicating that further increases in pile diameter yield only marginal increase in pile capacity. Similar behaviour was observed for model piles embedded in soil at different values of suction such as 0 kPa, 28 kPa, 893 kPa, 1211 kPa and 1716 kPa.

Figure 5(b) shows the percentage increase in the ultimate capacity of pile with respect to slenderness ratio for different suction values. The results demonstrated that the pile ultimate capacity consistently increased as the *l/d* ratio decreased from 62 to 31, with percentage increase showing a declining trend across all suction ranges. A maximum percentage increase of 8% to 12% was observed when l/d ratio decreased from 62 to 51.7 and minimum percentage increase of 3% to 5% was observed when l/d ratio further decreased from 34.4 to 31 across all suction ranges. These observations from Figure 5(a) and 5(b) demonstrates a geotechnical performance threshold where additional increase in pile diameter yielded marginal percentage increase in pile capacity. The observed behaviour was consistent with the findings of Borghi et al. (2001), who reported that both shaft and base resistance tend to saturate beyond a certain pile diameter due to limited additional mobilization of soil resistance.

© ASCE

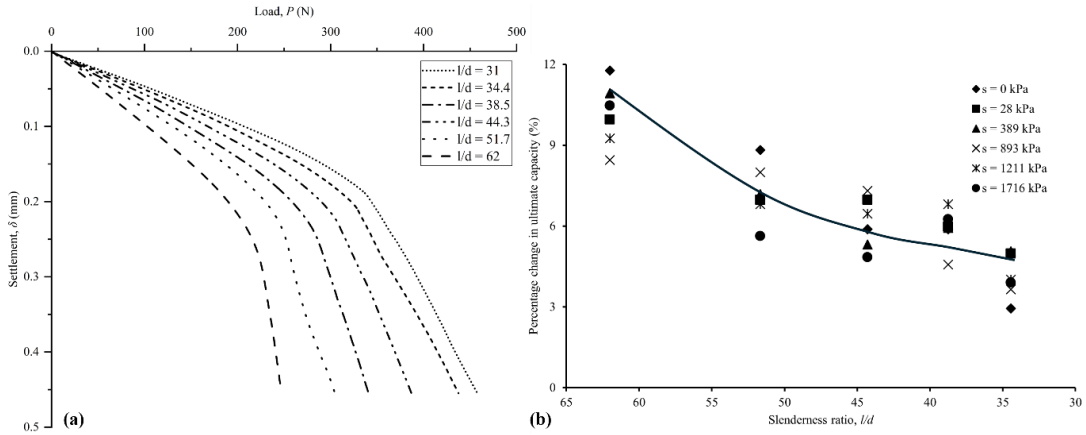


Figure 5. (a) Load settlement response of single pile under different slenderness ratio for suction = 389 kPa (b) Percentage increase in ultimate capacity with respect to slenderness ratio for different suction values

CONCLUSIONS

The present study analysed the influence of suction and pile geometry on the load-settlement response of the single pile embedded in unsaturated low plasticity clay using finite element code *numgeo*. A static steady state analysis approach was adopted to numerically simulate the pile response under different suction values and length to diameter ratios. The simulation results revealed that matric suction significantly improved the load-carrying capacity of model pile in unsaturated clays. The effect was particularly pronounced at lower suction values, where the pile capacity increased by 368% for 28 kPa of suction as compared to saturated condition. However, a marginal increase of 15% was observed in pile capacity as suction increased from 1211 kPa and 1716 kPa indicating the limited contribution of suction at residual zone of unsaturation. A similar trend was observed for the ultimate load capacity, where the percentage increase in ultimate capacity of pile decreased as suction increased beyond 1211 kPa, reflected by a noticeable reduction in the slope of ultimate capacity with respect to suction curve. In addition, the study emphasized the critical role of pile geometry, with a substantial increase in pile capacity was observed as the slenderness ratio decreased from 62 to 31 across all ranges of suction. However, a declining trend in the percentage increase in pile capacity was observed as l/d ratio reduced up to 31, with a minimum percentage increase of 3% to 5% observed when l/d ratio was reduced beyond 34.4, indicating further increase in pile diameter yield marginal increase in ultimate capacity of pile. Overall, the obtained results from numerical analysis showed the importance of considering unsaturated soil mechanics along with pile geometry into the design procedure for resilient and sustainable deep foundations.

REFERENCES

Abaqus. (2011). *Abaqus 6.11*. Dassault Systemes Simulia Corporation, Providence, RI, USA, 3, 73.

Achten, W. M., Trabucco, A., Maes, W., Verchot, L. V., Aerts, R., Mathijs, E., and Muys, B. (2013). Global greenhouse gas implications of land conversion to biofuel crop cultivation in arid and semi-arid lands–Lessons learned from Jatropha. *Journal of Arid Environments*, 98, 135-145.

© ASCE

Al-Khazaali, M., and Vanapalli, S. K. (2019). Experimental investigation of single model pile and pile group behavior in saturated and unsaturated sand. *Journal of Geotechnical and Geoenvironmental Engineering*, 145(12), 04019112.

Bishop, A. W. (1959). The principal of effective stress. *Teknisk ukeblad*, 39, 859-863.

Bishop, A. W., and Blight, G. E. (1963). "Some aspects of effective stress in saturated and unsaturated soils." *Géotechnique*, 13, 177–197.

BIS. (2013). Indian Standard Code of Practice for Design and Construction of Pile Foundations, IS 2911 Part 4: Load test on piles (First Revision), Manak Bhavan, 9 Bahadur Shah Zafar Marg, New Delhi 110002.

Borghi, X., White, D. J., Bolton, M. D., and Springman, S. (2001, April). Empirical pile design based on cone penetrometer data: an explanation for the reduction of unit base resistance between CPTs and piles. In *Proc. 5th Int. Conf. on Deep Foundations Practice, Singapore* (pp. 125-132).

Georgiadis, K., Potts, D. M., and Zdravkovic, L. (2003). The influence of partial soil saturation on pile behavior. *Géotechnique*, 53(1), pp.11-25.

Kumar, S., and Kumar, A. (2023a). Effect of Infiltration on Single-Pile and Monopile–Raft Foundation Embedded in Unsaturated Sand. *International Journal of Geomechanics*, 23(2), 04022288.

Kumar, S., and Kumar, A. (2023b). Behavior of Single Pile and Mono Pile-Raft Foundation under Hydraulic Loading Considering Hysteresis in Unsaturated Soils. In *Geo-Congress* (pp. 228-239).

Kumar, S., and Kumar, A. (2023c). Load transfer mechanism of single pile and mono-pile raft foundation in unsaturated sand. *Geo-Resilience 2023*, Cardiff, United Kingdom, March 28-29, 2023.

Kumar, S., Kumar, A., and Osman, A. (2025). Response of single pile in low expansive unsaturated clay subjected to hydraulic cycles: physical modelling, *Geotechnique Letters* (Under Review).

Lee, J., and Lee, J. (2025). Groundwater-Induced Settlements of Group Piles in Sand through Rising and Falling Phases of Groundwater Fluctuation. *International Journal of Geomechanics*, 25(5), 04025065.

Liu, Y., and Vanapalli, S. K. (2022). Modified shear displacement method for analysis of piles in unsaturated expansive soils considering influence of environmental factors. *International Journal of Geomechanics*, 22(6), 04022069.

Machacek, J., and Staubach, P. (2022). *numgeo*.

Nishimura, T., Toyota, H., Vanapalli, S. K., and Oh, W. T. (2008, October). The shear strength behavior of a silty soil in the residual zone of unsaturation. In *The 12th International Conference of International Association for Computer Methods and Advances in Geomechanics (IACMAG)* (pp. 2213-2221).

Oh, W. T., Vanapalli, S. K., and Puppala, A. J. (2009). "Semi-empirical model for the prediction of modulus of elasticity for unsaturated soils." *Can. Geotech. J.*, 46(8), 903–914.

Oh, W., and Vanapalli, S. (2013). "Interpretation of the bearing capacity of unsaturated fine-grained soil using modified effective and total stress approaches." *Int. J. Geomech.*,, 769–778.

Pham, T. A., Nadimi, S., and Sutman, M. (2024). Softening-based interface model and nonlinear load-settlement response analysis of piles in saturated and unsaturated multi-layered soils. *Computers and Geotechnics*, 171, 106331.

© ASCE

Poulos, H. G. (1989). Pile behaviour—theory and application. *Geotechnique*, 39(3), 365-415.
Sheikhtaheri, M. (2014). *Experimental and numerical modeling studies for interpreting and estimating the p–δ behavior of single model piles in unsaturated sands* (Doctoral dissertation, Université d'Ottawa/University of Ottawa).
Van Genuchten, M. T. (1980). "A closed-form equation for predicting the hydraulic conductivity of unsaturated soils." *Soil Sci. Soc. Am. J.*, 44, 892–898.
Vanapalli, S. K., Fredlund, D. G., Pufahl, D. E., and Clifton, A. W. (1996). "Model for the prediction of shear strength with respect to soil suction." *Can. Geotech. J.*, 33(3), 379–392.
Vanapalli, S., and Oh, W. (2010). A model for predicting the modulus of elasticity of unsaturated soils using the soil-water characteristic curve. *International Journal of Geotechnical Engineering*, 4(4), 425-433.
Vanapalli, S. K., Eigenbrod, K. D., Taylan, Z. N., Catana, C., Oh, W. T., and Garven, E. (2010, September). A technique for estimating the shaft resistance of test piles in unsaturated soils. In *Fifth International Conference Unsaturated Soils, UNSAT* (pp. 1209-1216).
Wheeler, S. J., Sharma, R. S., and Buisson, M. S. R. (2003). Coupling of hydraulic hysteresis and stress–strain behaviour in unsaturated soils. *Géotechnique*, 53(1), 41-54.
Wu, X., and Vanapalli, S. K. (2022). Three-dimensional modeling of the mechanical behavior of a single pile in unsaturated expansive soils during infiltration. *Computers and Geotechnics*, 145, 104696.

© ASCE